Indicators of Chaos

Manabu YUASA[1] *and* L. M. SAHA[2]
[1]*RIST, Kinki University, Higashi-Osaka 577-8502, JAPAN*
[2]*Department of Mathematics, Zakir Husain College, University of Delhi, New Delhi 110002, INDIA*

(Received 25 December, 2007)

Abstract

Chaotic phenomena are getting interest in all spheres of knowledge. In the past there were certain tools to identify regular and chaotic motions in dynamical systems such as time series curves, phase plots, Poincaré maps, power spectra, Lyapunov Exponents etc. These indicators, though very powerful, are not sufficient to differentiate regular and chaotic motion when the system bears higher degrees of freedom. Recent developments in nonlinear dynamics, provide some new tools like Fast Lyapunov Indicators (FLI), Smaller Alignment Indices (SALI), Dynamic Lyapunov Indicators, 0 - 1 test etc. to overcome this problem. These new tools are discovered and explained by various researchers. In the present article these new tools have been discussed and their applications have been shown with satisfactory answers. Burger's map, Chirikov map and Bouncing ball dynamics model are brought in this cotext. Results obtained are quite satisfactory and significant.

Key words: Indicators of chaos, Regular(Ordered) motion, Chaotic motion

1 Introduction

In nonlinear systems with higher degrees of freedom phase space is not clearly feasible and due to that the traditional indicators, like time series plots, phase plot, Poincaré map, power spectra etc, are in no way sufficiently qualified to identify ordered and chaotic behaviour. To over come this problem some new indicators have been discovered recently. ! ! Fast Lyapunov Indicator (FLI) was introduced by Froeschlé et al (1997), Smaller Alignment Indices (SALI) was introduced by Skokos ! J2001 ! Kand Skokos et al (2004). These indicators are now used by many researchers to identify chaotic and ordered motions originating in various systems. More recently, an another new indicator named as Dynamic Lyapunov Indicator (DLI) has been introduced by Saha and Mridula (2007) which gives very clear indication of ordered and chaotic motion whenever applied. All these indicators together with one more called 0 -#1 test, were used recently to study regular and chaotic motion in bouncing ball dynamics by Mridula et al (2007). Dynamics of bouncing ball has been reported by Everson in (1986). Since then this problem has attracted to many researchers such as Mello (1987), syta and Litak (2008). The 0 -#1 test was introduced by Gottwald and Melbourne (2004, 2005). Presently we have used this last indicator only when discussing bouncing ball dynamics. Also, it is to be mentioned that the 0 - 1 test results used here while discussing motion of the Bouncing ball is the reproduction of the work reported in a recent paper by Mridula et al (2007).

2 Indicators of Chaos

Herebelow, we have defined the four indicators of regularity and chaos as follows! '

(a! KFast Lyapunov Indicator (FLI):
Starting with an m-dimensional basis $V_m(0) = (v_1(0), v_2(0), \cdots, v_m(0))$, embedded in an n-dimensional space with an initial condition $(x_1(0), x_2(0), \cdots, x_n(0))$, we take at each iteration the largest amongst the vectors of the evolving basis. ! ! Thus, the FLI is defined as:

$$\text{FLI} = \sup \|v_j\|, j = 1, 2, \cdots, m \qquad (1)$$

It has been observed that *FLI's increase exponentially for chaotic orbits and linearly for regular orbits.*

(b! KSmaller Alignment Index (SALI):
First consider an n-dimensional phase space and an orbit in this space with initial condition P(0) $= (x_1(0), x_2(0), \cdots, x_n(0))$, and a deviation vector $\xi(0) = (dx_1(0), dx_2(0), \cdots, dx_n(0))$ for the initial point P(0). To compute the SALI for a given orbit, we follow the time evolution of the orbit of P(0) together with two deviation vectors $\xi_1(t), \xi_2(t)$ which initially point in two different directions in the phase space. At every time step the two deviation vectors $\xi_1(t), \xi_2(t)$ are normalized and the SALI is then defined as follows:

$$\text{SALI} = min \left\{ \| \frac{\xi_1(t)}{\|\xi_1(t)\|} - \frac{\xi_2(t)}{\|\xi_2(t)\|} \|, \right.$$

$$\left. \| \frac{\xi_1(t)}{\|\xi_1(t)\|} + \frac{\xi_2(t)}{\|\xi_2(t)\|} \| \right\} \qquad (2)$$

It is found that *the SALI fluctuates around a non-zero value for ordered orbits while it tends to zero for chaotic orbits.*

For both the FLI and the SALI we evolve the vectors by applying to them the evolving Jacobian matrix at each iteration for a discrete system.

(c)Dynamic Lyapunov Indicator (DLI):
The dynamic Lyapunov indicator (DLI) is defined by the largest value estimated from all eigenvalues λ_j of the Jacobian matrix J such that

$$\text{J} - \lambda_j I = 0;$$

$$j = 1, 2, \cdots, n \text{ (for n-dimensional map)} \qquad (3)$$

of the examined map for all discrete times. *If these eigenvalues form a definite pattern, then the motion is regular and if they are distributed randomly, (with no definite pattern), then the motion is chaotic.*

(d) 0-1 Test:
This $0-1$ test can be applied to any system with finite dimension, but it is based only on the statistical property of a single coordinate of the system. ! ! The reliability of this test is established by Jing Hu et al (2005). We define and explain this test as follows:
Starting with $x_k(i)$ as one of the initial coordinate, $k \in \{1, 2, 3, \cdots, n\}$, we define new coordinates $p(n), q(n)$ as

$$\begin{aligned} p(n) &= \sum_{j=1}^{n} x_k(j) \cos(nc) \\ q(n) &= \sum_{j=1}^{n} x_k(j) \sin(nc) \end{aligned} \qquad (4)$$

Here, $q(n)$ is the complementary coordinate in 2 - D space and c is chosen arbitrarily (in case of bouncing ball we assumed c=1.7). Thus, starting with bounded coordinate $x(i)$, we construct a series of $p(n)$ which can be either bounded or unbounded depending on the dynamics of the process to be examined.
For a given periodic series $x_k(i)$,

$$\Gamma(n) = x_k(n) cos(nc)$$

represents the random number as

$$p(n+1) = p(n) + \Gamma(n),$$

and total mean square displacement is scaled on n. On the other hand for a periodic or quasi-periodic signal

$$x_k(i+L) = x_k(i) \text{ or } x_k(i+L) \approx x_k(i),$$

where L is a period, the total mean square displacement is 0. So, any chaotic vibration in the

initial space x corresponds to an unbounded motion in (p, q) plane while a regular vibration in x is related to the bounded motion in this plane. For qualitative description of the examined solution one calculates the asymptotic properties defined as the total mean square displacement

$$M(n) = \lim_{n\to\infty} \frac{1}{n} \sum_{j=1}^{n} (p(j+n) - p(n))^2 \qquad (5)$$

Finally, we obtain the control parameter K in limit of a very long time

$$K = \lim_{n\to\infty} \frac{\ln(M(n)+1)}{\ln n} \qquad (6)$$

In the case of 0 - 1 test, the velocity v, (or v_n) can be used, as the starting coordinate $x_k = v$ and obtain the set of (p, q) coordinates through eqn (4). Then, the corresponding trajectories in this plane can be plotted as phase portrait. For the case of bouncing ball, an unbounded drift has been observed for a chaotic solution and a motion around a certain circle (or curve) in case of regular motion as shown in Fig.1, (a) for chaotic motion and (b) for regular motion.

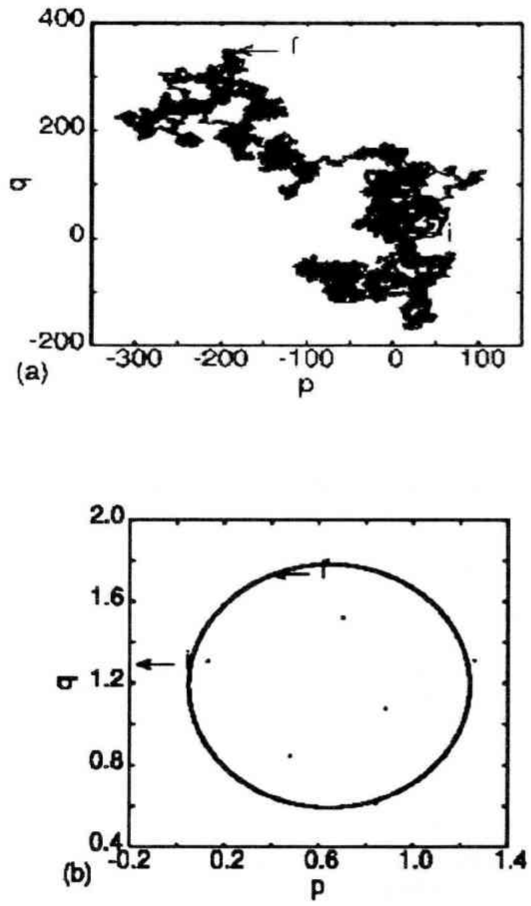

Fig.1. Phase portrait of bouncing ball problem: Figure(a) represents the chaotic case while (b) represents the regular case.

3 Application of above Indicators

We have applied above defined indicators in the models given below:

(i) Burger's Map:

$$\begin{aligned} x_{n+1} &= (1-a)x_n - y_n^2 \\ y_{n+1} &= (1+b)y_n + x_n y_n \end{aligned} \tag{7}$$

where a and b are non-zero parameters . This map evolve chaotically when a=0.9, b=0.856. To control chaotic motion we have used pulsive feedback control technique, Litak et al (2007) by changing the above map slightly as

$$\begin{aligned} x_{n+1} &= (1-a)x_n - y_n^2 + \epsilon(x+0.856) \\ y_{n+1} &= (1+b)y_n + x_n y_n + \epsilon(y-0.87772433) \end{aligned} \tag{8}$$

Here (-0.856, 0.87772433) is an unstable fixed point of the original Burger's map. It has been observed that for , $\epsilon = -0.3$! ! above chaotic motion gets controlled and display regular behaviour. This can be observed through the phase plots given in Fig.2.

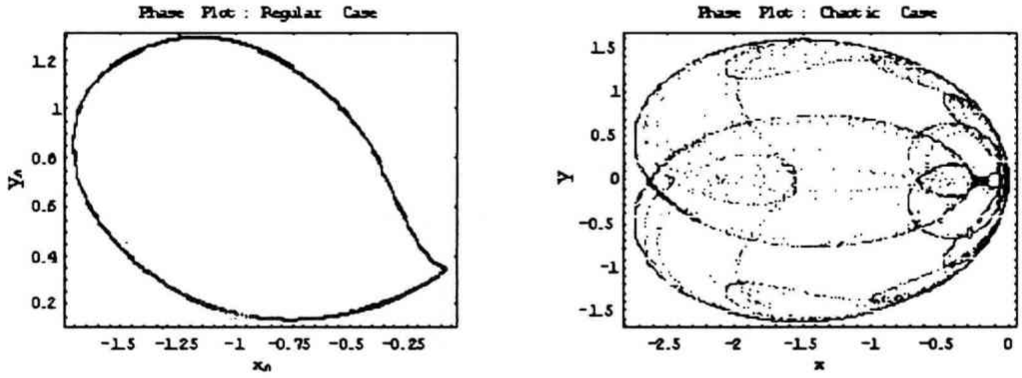

Fig.2. Phase plots of ! ! Burger's map for a = 0.9, b = 0.856 and ϵ ! a -0.3 when regularized and shown here in the left plot.

For this map FLI, SALI and DLI are computed respectively and displayed through the following plots:

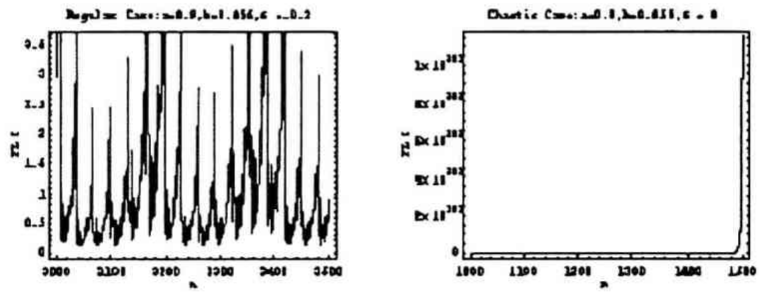

Fig.3. FLI plots for regular and chaotic cases of Burger's map.

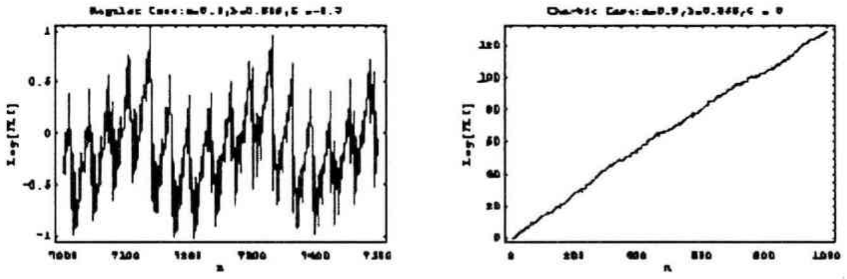

Fig.4. Log[FLI] plots for regular and chaotic motions in Burger'map

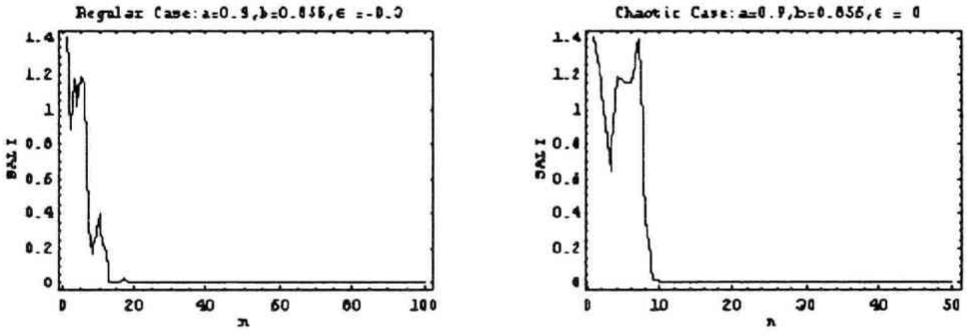

Fig.5. SALI plots for regular and chaotic motions in Burger's map

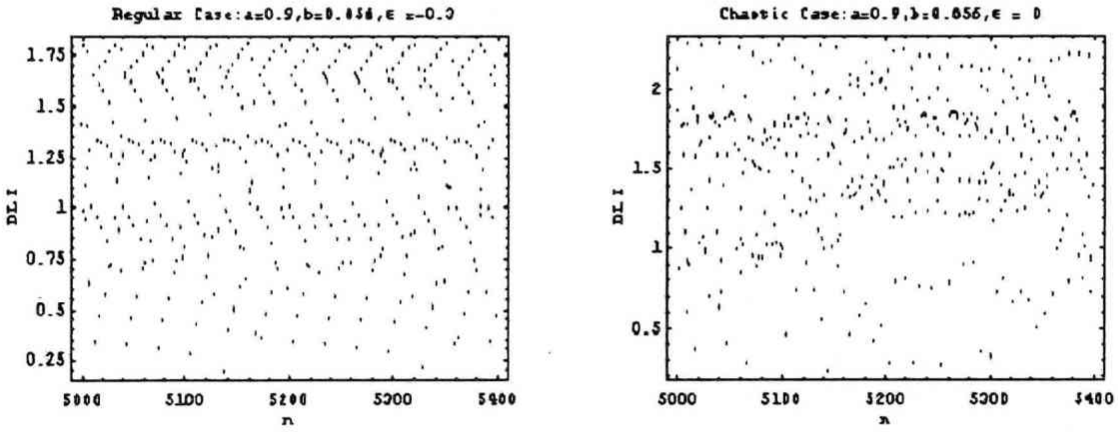

Fig.6. DLI plots for regular and chaotic evolution of Burger's map. A pattern is clearly visible for the regular case.

(ii) Chirikov Map:

! !

$$\begin{aligned} x_{n+1} &= x_n - k \sin y_n \mod(2\pi) \\ y_{n+1} &= y_n + x_{n+1} \mod(2\pi) \end{aligned} \tag{9}$$

This map evolve chaotically when $k = 2.5$ and it is regular when $k = 0.5$. Phase plots for these cases are shown in Fig.7 as

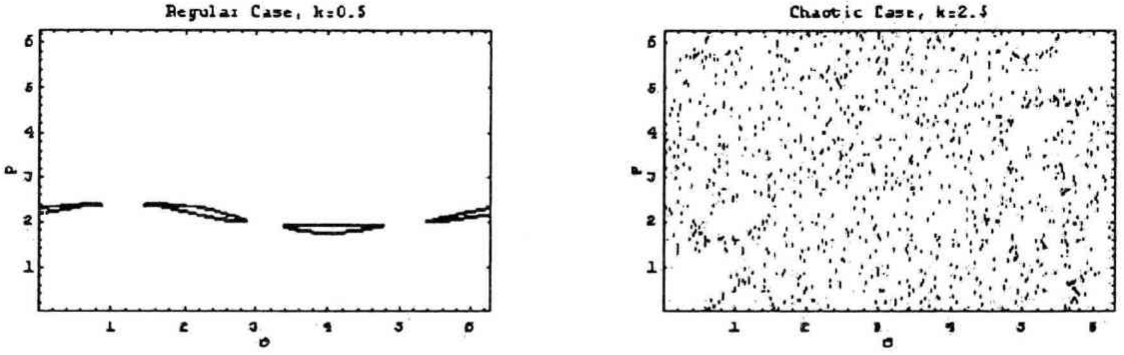

Fig.7. Phase plots of Chirikov Map.

The following plots are those of FLI, SALI and DLI for this map given through figures Fig. 8 - Fig. 10.

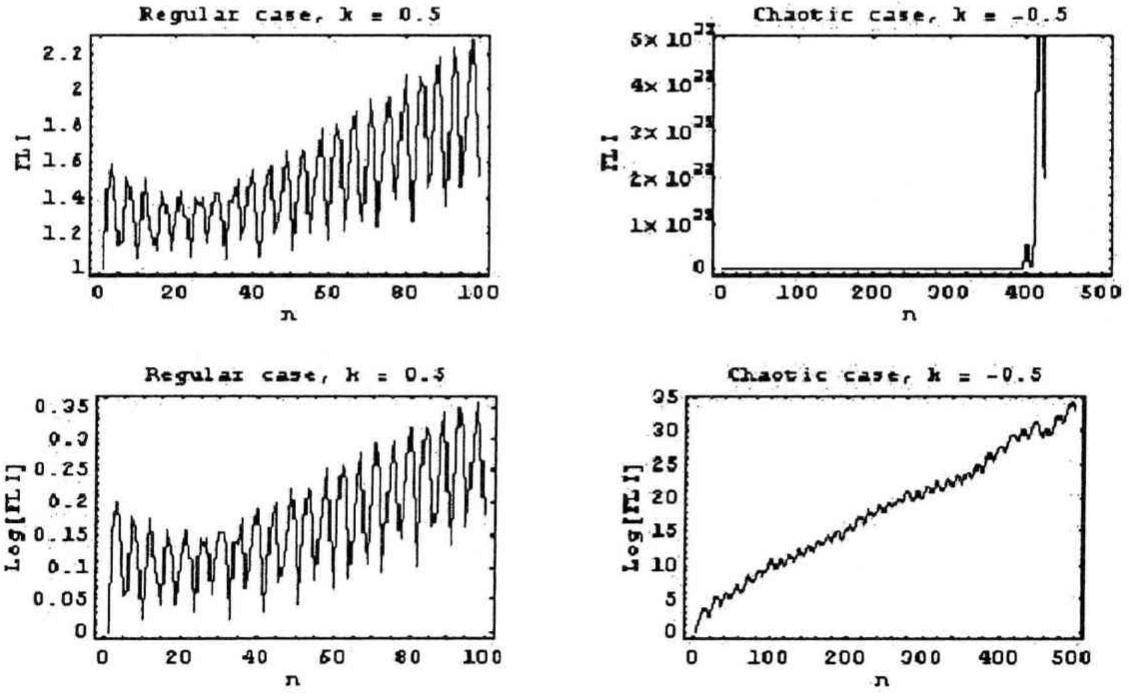

Fig.8. FLI and Log[FLI] plots of Chirikov Map.

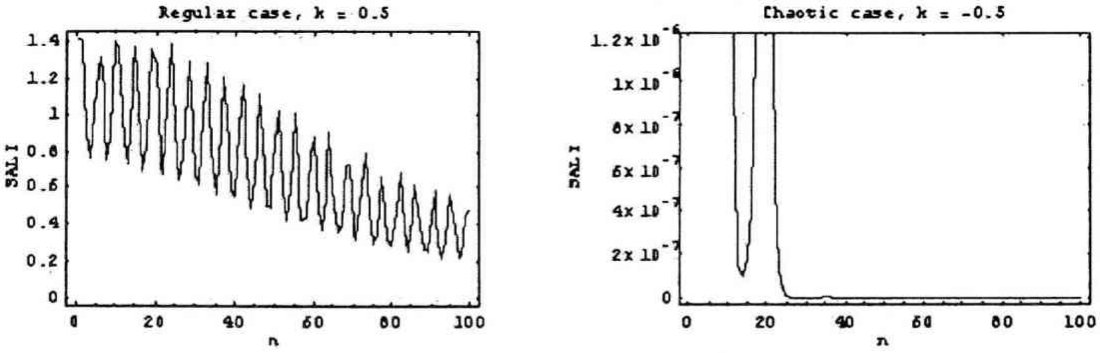

Fig.9. SALI plots of Chirikov map.

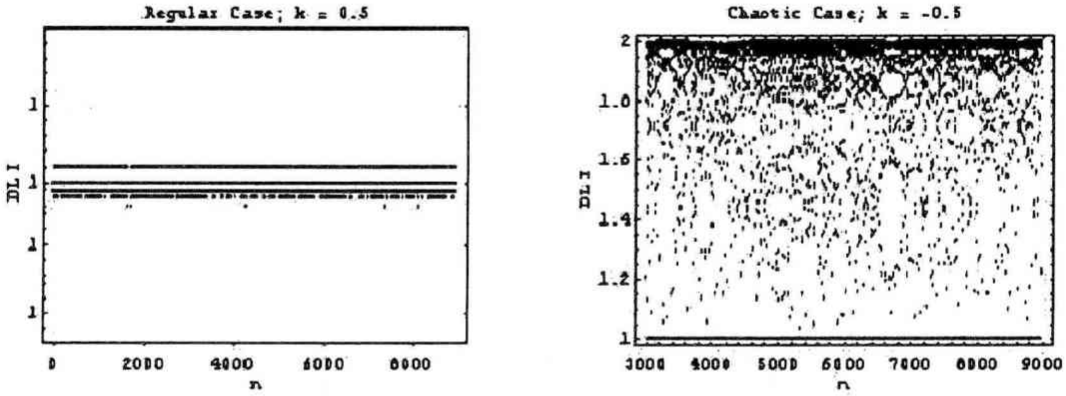

Fig.10. DLI plots of Chirikov map. The figure on the right side indicates the transition from regular to chaotic motion.

4 Bouncing Ball Problem

Dynamics of bouncing ball has been reported in a recent research work by Mridula et al (2007). The forgoing discussion is nothing but the work done by them which has certain significance in context of this paper. In the figure below we have a bouncing ball in the Earth gravitational field impacting a harmonicaly oscillating plate.

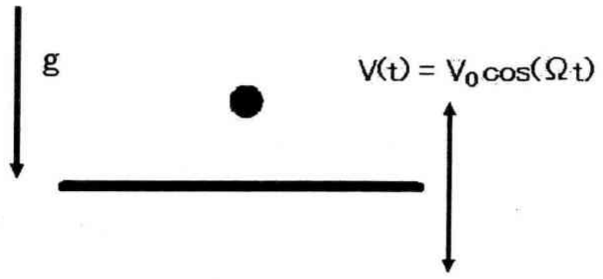

Fig.11. Bouncing ball model

A map for velocities and impact instants $-v_n$ and t_n, respectively, can be expressed by the following set of difference eqn :

$$\begin{aligned} &V_{n+1} = -k(v_n - \mathrm{g}\triangle t_n) \\ &+(1+k)V_0\cos(\Omega t_{n+1}) \\ &V_0/\Omega(\sin(\Omega t_{n+1}) - sin(\Omega t_n) \\ &= v_n\triangle t_n - \mathrm{g}/2(\triangle t_n)^2, \end{aligned} \tag{10}$$

where $\triangle t$ be the time interval between impacts and k represents the restitution coefficient and < 1, ! !(Tél and Gruiz,2006). Introducing phase $\phi_n = \Omega t_n$, one gets the following simplified dimensionless map:

$$\begin{aligned} &\phi_{n+1} = \phi_n + \triangle\phi_n \\ &v_{n+1} = -k(v_n - 2\triangle\phi_n/q) \\ &+(1+k)\cos\phi_{n+1}, \end{aligned} \tag{11}$$

where the phase difference $\triangle\phi_n$ can be obtained from eqn

$$\sin(\phi_n + \triangle\phi_n) - \sin\phi_n = v_n\triangle\phi_n - 2\triangle\phi_n/q. \tag{12}$$

Here $q = 2V_0\Omega/\mathrm{g}$ is the dimensionless driving frequency. In the limit when $q >> 1$, above equation reduces to

$$\begin{aligned} &\phi_{n+1} = \phi_n + \triangle\phi_n \\ &v_{n+1} = v_n + (1+k)\cos\phi_{n+1}, \end{aligned} \tag{13}$$

As shown in Fig.1, phase portrait for this map, appears to be chaotic when q= 20.0, $k = 0.3$ and regular when $q = 2.0$ and $k = 0.3$. For quantitative analysis we have estimated the $M(n)$ by using eqn (5). To show the asymptotic behaviour, we have plotted $\ln M(n)$ against $\ln n$. In both cases we obtained linear dependence,

$$\ln M(n) = \tan\Psi \ln n + c_i, \quad i = a, b. \tag{14}$$

This is shown through the figure Fig.12.

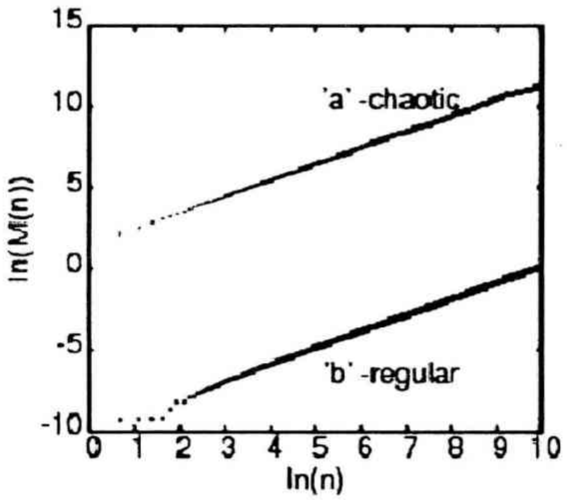

Fig.12. Plot of $\ln M(n)$ versus $\ln n$.

In (14), Ψ is the slope, dependent on a c-parameter value and same for both lines while c_a, c_b. ! !Note that $c_a > 0$ while $c_b < 0$. These determine $M(n)$ dependence on n and we have $M(n) = n^\alpha e^{c_i}$, where $\alpha = \tan\Psi$. Clearly for positive c_i, M scales much stronger with n^α then for a negative c_i. Furthermore, from above figure, one can also conclude that for the case of the b-solution and in the limit of large n,

$$\ln M(n) \to 0 \quad \text{for large } n.$$

! ! ! ! Evidently, this constraint is strictly connected with the negative value of c_b, namely $c_b \approx -\ln n$. ! ! Such differences in scaling are crucial in determining the value of K. Conse-

quently, having $M(n)$, we obtained $K = 0.925$ for the chaotic series and $K = 0.042$ for the periodic one. It is clear enough that the parameter K tends to 1 for the chaotic solution while 0 for a regular solution. In the calculation by Mridula et al (2007), they used $N = 20000$ and $n = 180000$ respectively.

For evolutionary behavior of bouncing ball map in context of FLI, SALI and DLI we have following plots for regular and chaotic cases indicated there:

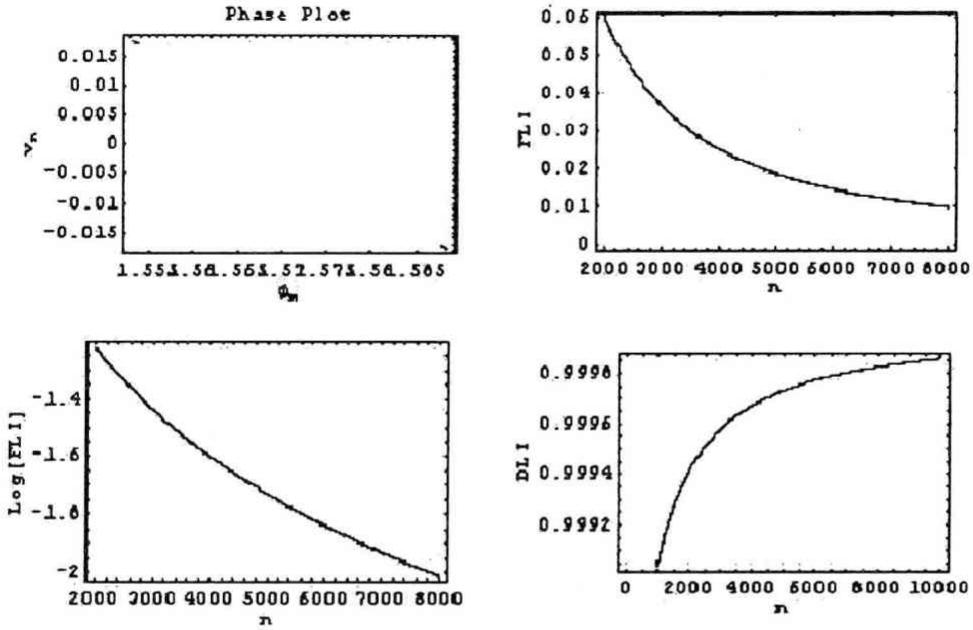

Fig.13. Phase plot and FLI, log[FLI] and DLI plots of bouncing ball dynamics when the motion is regular.

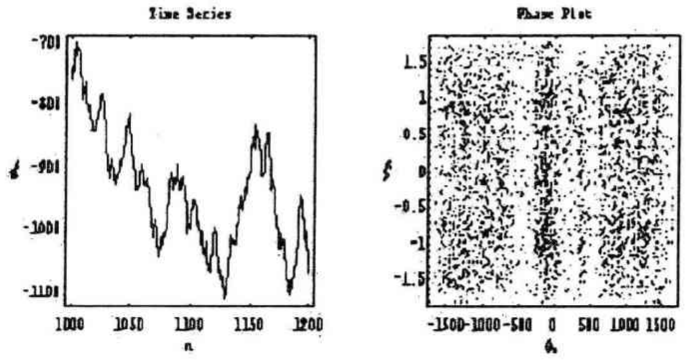

Fig.14. Phase plot for chaotic motion.

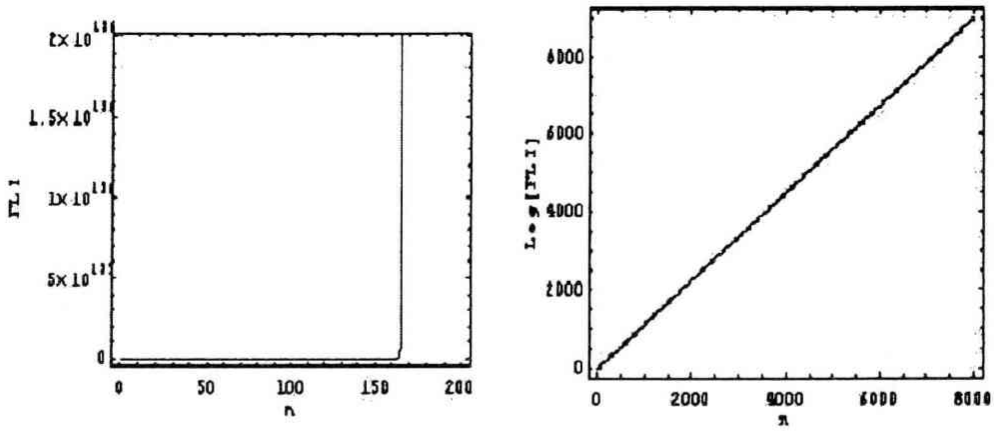

Fig.15. FLI and log(FLI) plots.

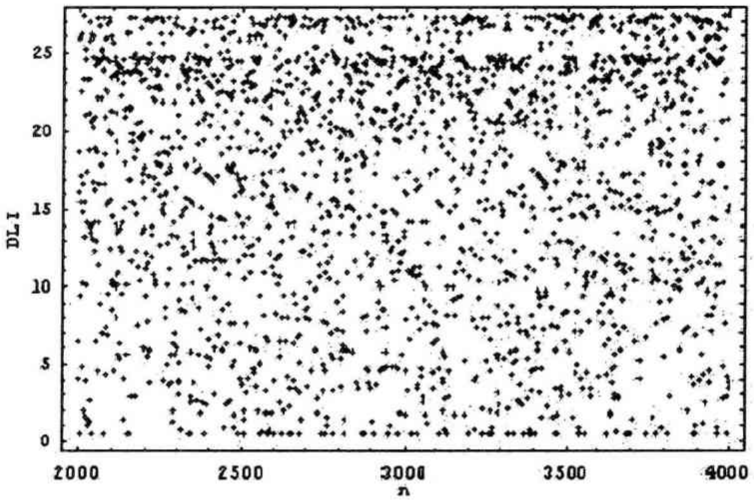

Fig.16. DLI plot for chaotic motion.

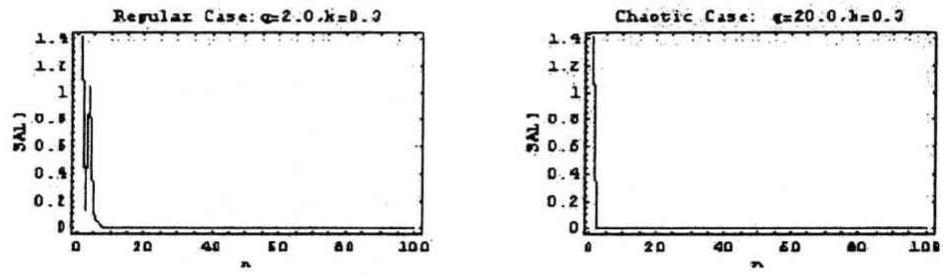

Fig.17. SALI plots for regular and chaotic motion.

5 Brief Discussion

From above numerical results it has been noticed that for 2-dimensional cases SALI do not provide a clear picture of identification of regular and chaotic motion, DLI provides a clear picture for all maps. Also 0 - 1 test has its own merit for qualitative analysis. These methods of identification can be applied to other discrete maps also. It is to be important to verify these for continuous maps also.

Acknowledgement

L. M. Saha is supported by JSPS for his visit to Kinki University, Osaka. During his visit this work has been prepared. We are grateful to Emeritus Prof. W. Unno of the University of Tokyo for valuable discussions.

References

[1] Everson R.M.1986: Chaotic dynamics of a bouncing ball. Physica D, 19, 355-383

[2] Mello T.M. 1987): Strange attractors of a bouncing ball. Am. J. Phys., 55, 316 - 320

[3] Saha L.M. and Mridula Budhraja 2007: The largest eigenvalue! 'An indicator of chaos? IJAMM, 3(1), 61 - 71

[4] Saha L.M., Das M.K. and Mridula Budhraja 2006: Characterization of attractors in Gumowski-Mira map using fast Lyapunov indicator., FORMA 21, 151 - 154

[5] Mridula Budhraja 2007: On Synchronization, Control and Characterization of Chaos in Dynamical Systems. Ph.D. Thesis, submitted to the University of Delhi.

[6] Mridula Budhraja, Syta A., Saha L.M. and Litak G. 2007: Bouncing ball dynamics by novel chaos indicators, Preprint submitted to Elsevier.

[7] Froeschlé C, Gonczi R. and Lega E. 1997: The Fast Lyapunov Indicator: A simple tool to detect weak chaos, Application to the structure of the main asteroidal belt. Space Sci. 45, 881 - 886

[8] Lega E. and Froesschlé C. 2002: On the relationship between Fast Lyapunov Indicator and Periodic orbit symplectic mappings. Celet Mech. And Dyna. Astronomy, 81, 129 - 147

[9] Skokos Ch 2001: Alignment indices: a new simple methodfor determining the ordered or chaotic nature of orbits? J. Phys. A: Math Gen., 34, 10029 - 10043

[10] Skokos ch, Antonopoulos ch, Bountis T.C. and Vrahatis M.N. 2004: Detecting order and chaos in Hamiltonian systems by SALI method. J. Phys. A: Math. Gen. 37, 6269 - 6284

[11] Gottwald G. and Melbourne I. 2004: A new test for chaos in deterministic systems. Proc. R. Soc. Lond. A, 460, 603 - 611

[12] Gottwald G.A. and Melbourne I. 2005: Testing for chaos in deterministic systems with noise. Physica D, 212, 100 - 110

[13] Litak G., Borowiec M., Ali M., Saha L.M. and Friswell M.I. 2007: Pulsive feedback control of a quarter car forced by a road profile. Chaos Soliton and Fractals, 33, 1672-1676

[14] Jing Hu, Wen-wen Tung, J. B. Gao and Yinhe Cao 2005: Reliability of the 0 - 1 test for chaos. Phys. Rev. E 72, 056207.

[15] A syta and Litak G. 2008 : Description of the deterministic Ricker's population model. Chaos, Solitons & Fractals (in Press)

[16] Tél T. and Gruiz M. 2006 : Chaotic Dynamics, Cambridge ! ! Univ. Press.